Nailfold Capillaroscopy Capillaries Segmentation

Group Members

Qadeem Khan
Syed Sameed Ahmed

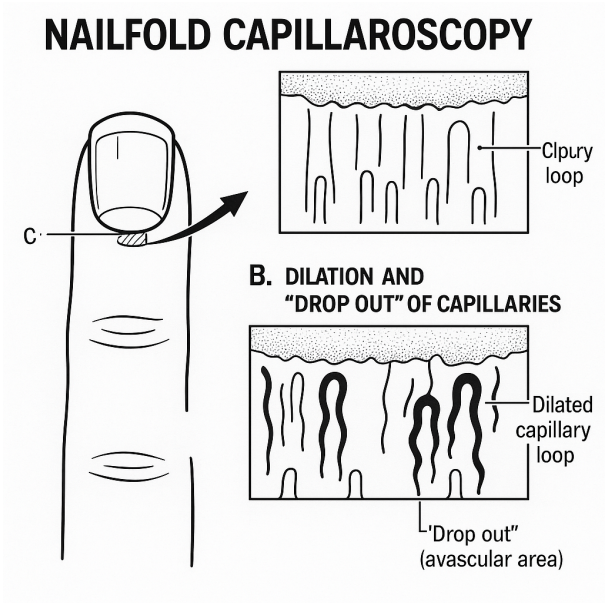

Submitted To

Prof. Dr. Stephanie Bricq

Computer Vision and Robotics

Université Bourgogne Europe

June 9, 2025

Contents

List of Figures

1 Abstract

Nailfold capillaroscopy is a non-invasive diagnostic imaging technique widely used to evaluate microvascular abnormalities, particularly in autoimmune and connective tissue diseases. This project presents a novel image processing-based methodology for detecting and counting capillaries in nailfold images without the use of machine learning or deep learning techniques. Leveraging classical computer vision algorithms, the method focuses on three sequential stages: preprocessing, enhancement, and capillary detection. Preprocessing involves the selection of the green color channel, Gaussian blurring, Canny edge detection, and Hough transform to isolate the region of interest (ROI) and correct for image rotation. The enhanced ROI is processed using histogram equalization and Contrast Limited Adaptive Histogram Equalization (CLAHE), adapted dynamically to the image's luminance. Capillary detection is achieved through morphological operations, thresholding, and geometric analysis of contours. Ellipse fitting and orientation assessment are used to classify tubular capillary shapes while excluding horizontal structures. Further refinements include proximity and orientation checks between contours to avoid overcounting. The method was tested on a dataset of 30 images from both healthy and diseased individuals, demonstrating reliable segmentation performance under diverse illumination and deformation conditions. Despite some limitations related to image quality and labeling accuracy, the approach successfully highlights the potential of traditional techniques in robust medical image analysis where machine learning may be impractical or unnecessary.

2 Introduction

Nailfold capillaroscopy (NFC) is a widely recognized, non-invasive imaging technique used to assess microvascular health by visualizing capillaries in the nailfold region. It plays a crucial role in the early diagnosis and monitoring of systemic conditions such as scleroderma, lupus, and other connective tissue diseases. The morphological features of capillaries—such as their shape, size, and density—serve as significant biomarkers in clinical assessments, often preceding other physiological symptoms.

The accuracy and efficiency of capillary assessment are critical in both research and clinical settings. Traditionally, this process has relied heavily on manual inspection, which is inherently subjective and labor-intensive. Automated approaches have gained traction, particularly those leveraging machine learning (ML) and deep learning (DL). However, despite their performance advantages, such models are often limited by their dependence on extensive annotated datasets, lack of interpretability, and high computational demands.

In light of these limitations, there is a growing interest in exploring alternative methodologies that do not rely on ML or DL. Classical image processing techniques offer a transparent and resource-efficient pathway for analyzing biomedical images, especially in contexts where computational or data resources are limited. These techniques, when thoughtfully integrated, can deliver consistent and explainable results, making them particularly suitable for routine medical imaging applications.

This report presents a methodological framework for capillary detection and quantification based exclusively on traditional image processing principles. The proposed approach emphasizes robustness, adaptability, and interpretability, aiming to contribute a practical solution to the domain of medical image analysis.

3 Problem Statement

In this project, the central problem addressed is the development of a robust, interpretable, and machine-learning-free methodology capable of reliably detecting and counting capillaries in nailfold images. The solution must account for the diverse challenges posed by real-world data, including inconsistent lighting conditions, rotated frames, and the structural differences between healthy and diseased capillaries.

The dataset used in this study consists of 30 nailfold images categorized into four groups: two representing healthy individuals (N1 and N2) and two from individuals with capillary abnormalities (S1 and S2). These images were intentionally selected to reflect a wide range of conditions, enhancing the complexity of the task and underscoring the need for a versatile and accurate image processing pipeline.

4 Methodology

The methodology is designed to be transparent, interpretable, and robust across varied image conditions, including changes in illumination and orientation. The pipeline is composed of three main phases:

1. Preprocessing
2. Processing
3. Analysis and counting.

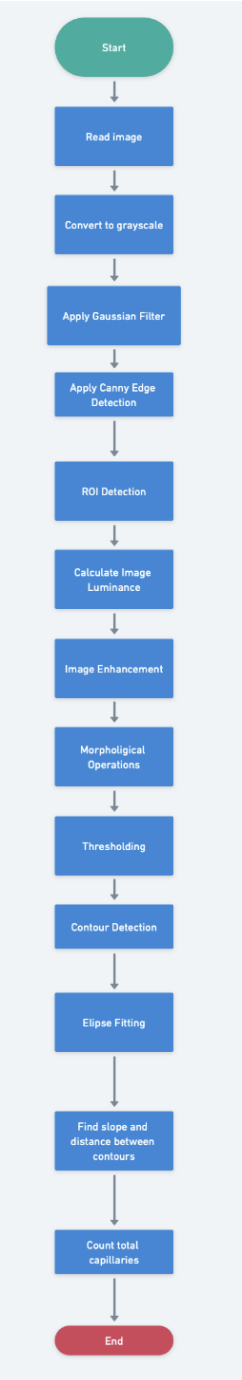

Figure 1: Methodology Flowchart

4.1 Preprocessing

The preprocessing stage prepares each image for capillary analysis by enhancing its interpretability and defining a region of interest (ROI) with high capillary density.

4.1.1 Channel Selection

Each input image is initially processed by extracting the green channel, which provides the best contrast for visualizing capillaries in nailfold images due to the typical absorption characteristics of blood vessels.

4.1.2 ROI Detection

To isolate the relevant area for capillary detection following steps are followed:

1. A Gaussian blur is applied to suppress image noise and smoothen fine details.
2. Canny edge detection is then used to extract the prominent edges in the image.
3. A Hough line transform is performed to detect linear structures. The longest detected line is assumed to align with the nailfold edge and is used as a reference to rotate the image for alignment.
4. Based on this orientation, a region of interest (ROI) is extracted, focusing on the central area where capillaries are most likely to be found.

4.2 Processing

The processing stage enhances the visual quality of the ROI and applies segmentation techniques to isolate candidate capillary structures.

4.2.1 Image Enhancement

To improve capillary visibility under different lighting conditions:

1. Histogram Equalization is applied to globally enhance contrast.
2. Contrast Limited Adaptive Histogram Equalization (CLAHE) is then used to improve local contrast, particularly in poorly illuminated images.
3. A luminance threshold is applied: if the average luminance is below 88, a more aggressive enhancement is triggered to compensate for low visibility.

4.2.2 Capillary Segmentation

Following steps are followed for the segmentation process:

1. A sequence of morphological operations (such as dilation and erosion) is applied to emphasize tubular structures and suppress irrelevant noise.
2. Thresholding techniques convert the image to binary format for structural analysis.
3. Contour detection is used to identify potential capillaries within the enhanced ROI.

Analysis and Counting

This stage involves evaluating the geometric and spatial characteristics of the detected contours to determine valid capillaries and accurately count them.

4.2.3 Geometric Filtering

Each contour is analyzed using ellipse fitting. Capillaries are expected to exhibit a tubular shape. If the fitted ellipse has a major axis angle near 90 degrees, the contour is classified as horizontal and excluded, since capillaries typically follow a vertical or diagonal orientation.

4.2.4 Proximity and Orientation Matching

To avoid overcounting:

1. The algorithm calculates the centroids of all valid contours.
2. Euclidean distance and slope between centroids are measured.
3. Contours with a slope between 0.5 and 1.5, and a distance below a defined threshold, are considered part of the same capillary. This accounts for slight segmentation artifacts where one capillary is split into multiple pieces.

This multi-stage, rule-based method ensures that the capillary count reflects biologically meaningful structures while maintaining computational simplicity and interpretability.

5 Implementation Results

The methodology was implemented entirely using classical image processing techniques in Python, relying on libraries such as OpenCV, scikit-image, and NumPy.

5.1 Preprocessing

Preprocessing begins by selecting the green channel from the RGB images, which best emphasizes capillary contrast. A Gaussian blur is applied to reduce noise before edge detection. The orientation of the capillary bed is estimated using Hough Line Transform, identifying the longest horizontal structure as the nailfold baseline.

Using the dominant line angle, the image is rotated to horizontal alignment, and a Region of Interest (ROI) is extracted below this line:

- ROI height: 210 pixels for healthy subjects (N1/N2),
- ROI height: 150 pixels for diseased subjects (S2/S3),

This ensures the consistent framing for capillary structures.

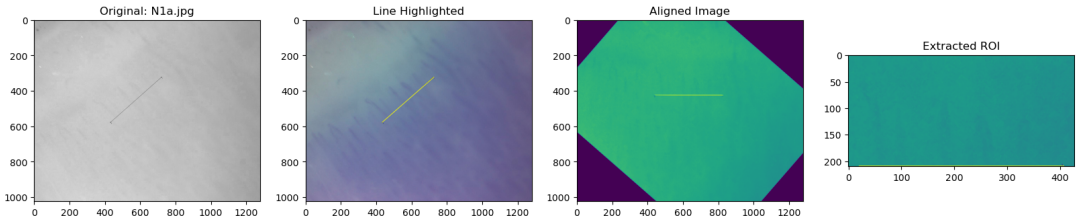

Figure 2: ROI Extraction Pipeline

Extracted ROI are displayed along with the original images for visual verification. This process is done for the images in the dataset

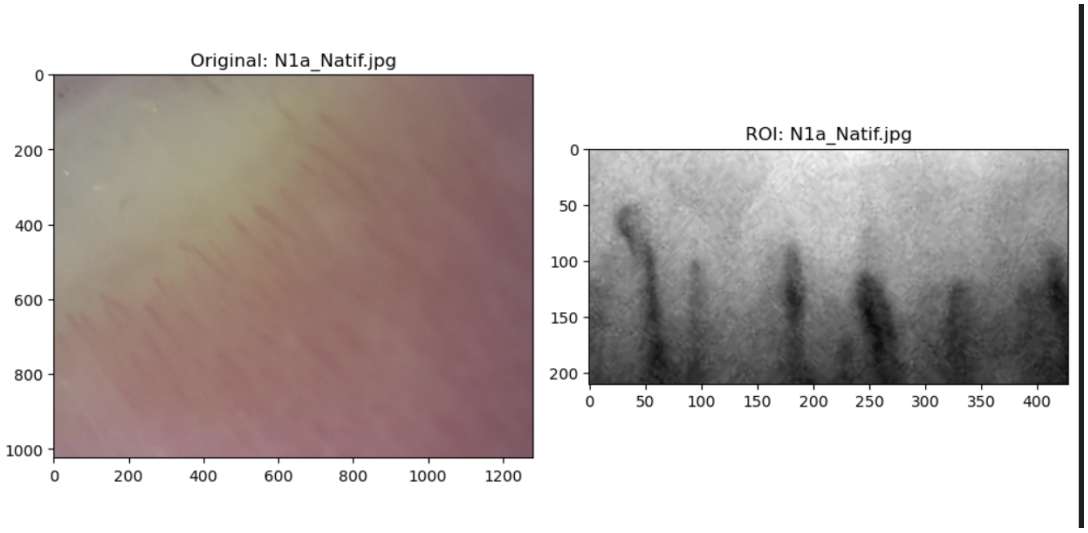

Figure 3: Original Image vs Extracted ROI

5.2 Image Enhancement and Segmentation

During the processing stage, the average luminance of each image was computed and used as a criterion to adapt enhancement intensity. For example, images with luminance below 88 underwent more aggressive CLAHE and adaptive thresholding to compensate for low contrast. This decision rule was critical for ensuring consistent processing across both well-lit and dimly lit images.

Table 1 presents a selection of computed luminance values across the dataset:

Table 1: Luminance values of images

Image	**Luminance**
N1b_Natif	124.46
N1d_Natif	122.28
N1i_Natif	96.95
N1c_Natif	129.33
N1e_Natif	92.78
N1h_Natif	117.48
N1f_Natif	106.25
N1a_Natif	140.32
N1g_Natif	106.25
N1j_Natif	102.93
N2c_Natif	79.30
N2d_Natif	74.48
N2b_Natif	65.21
S2d_Natif	154.72
S2b_Natif	215.37
S2e_Natif	202.81
S2c_Natif	216.01
S2f_Natif	208.72
S2g_Natif	190.16
S2a_Natif	199.92
S3f_Natif	83.97
S3a_Natif	93.62
S3g_Natif	64.51
S3j_Natif	76.04
S3b_Natif	87.89
S3d_Natif	84.12

Image	Luminance
S3i_Natif	73.84
S3c_Natif	77.30
S3e_Natif	69.30
S3h_Natif	50.62

Histogram Equalization adjusts global brightness distribution. Contrast Limited Adaptive Histogram Equalization (CLAHE) enhances local features with intensity based on image luminance:

- If average luminance ¡ 88: CLAHE with clipLimit = 5.0, followed by adaptive thresholding.
- Otherwise: CLAHE with clipLimit = 20.0, focusing on contrast expansion.

Following enhancement, adaptive Gaussian thresholding converts the image to binary, isolating high-intensity (likely vascular) structures.

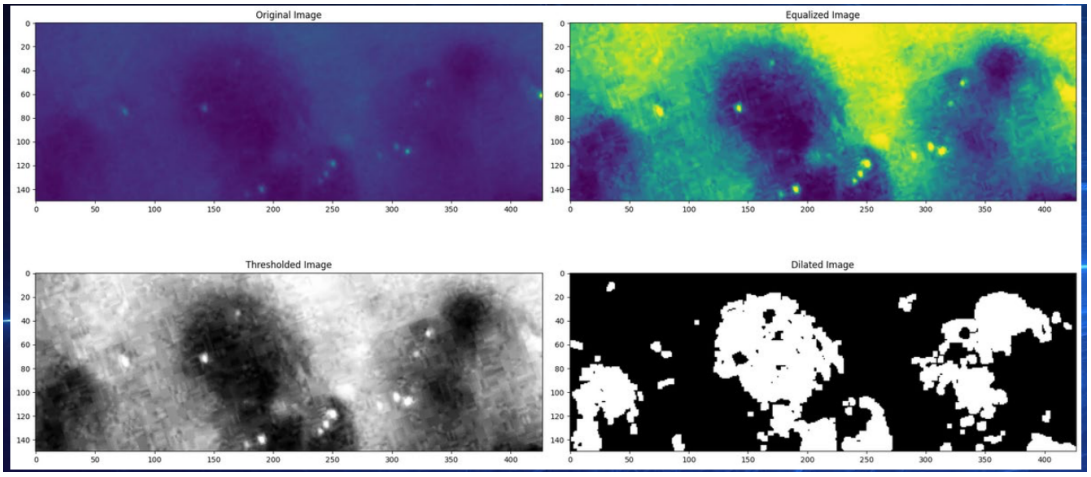

Figure 4: Histogram Equalization

Figure 4 illustrates the transformation of a Region of Interest (ROI) image through the enhancement and segmentation stages of the pipeline. Each sub-image demonstrates a distinct phase of processing, sequentially contributing to the accurate isolation of capillary structures:

1. Original Image (Top Left) The raw ROI is first extracted after rotation and alignment. Due to suboptimal illumination and background tissue texture, the capillary structures are not clearly visible in this form. Their visibility is further hampered by low local contrast and luminance variability, which necessitates enhancement.

2. Equalized Image (Top Right) This panel shows the effect of applying Contrast Limited Adaptive Histogram Equalization (CLAHE). This operation improves the visibility of faint capillaries by enhancing local contrast without oversaturating already bright areas. CLAHE dynamically adapts based on image luminance, making it particularly useful for capillaroscopy images with uneven lighting.

3. Thresholded Image (Bottom Left) After contrast enhancement, the image undergoes adaptive Gaussian thresholding. This method creates a binary-like output where pixels are segmented into foreground and background based on localized intensity patterns. The thresholded image begins to reveal potential capillary regions as bright elongated segments.

4. Dilated Image (Bottom Right) To ensure connectivity and minimize fragmentation in segmented capillaries, morphological dilation is applied. This step expands the detected structures, connecting nearby regions and suppressing small noise. The output is a binary mask where candidate capillaries appear as white regions, preparing the image for contour extraction and shape-based filtering.

6 Morphological Processing and Contour Extraction

Following enhancement and segmentation, the binary image undergoes a series of morphological transformations designed to refine capillary-like structures and suppress irrelevant noise. These operations serve as a crucial bridge between thresholding and the final analytical stage of capillary counting.

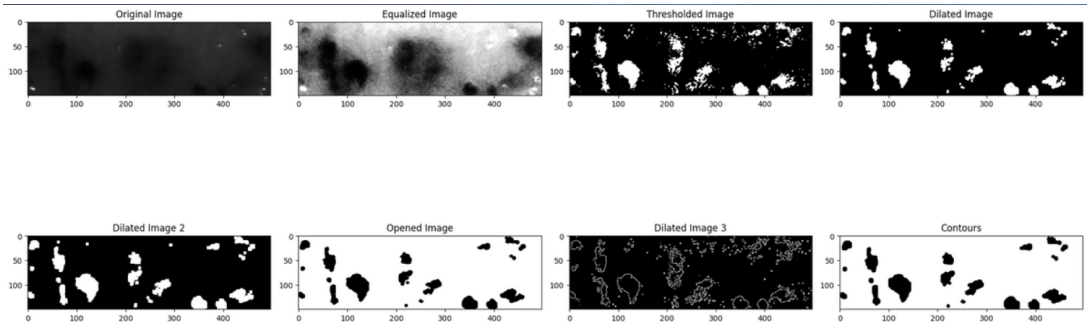

Figure 5: Morphology Operations

The process begins with morphological dilation, which is used to expand foreground regions in the thresholded image. This helps to connect disjointed or weakly segmented parts of capillaries, ensuring the structural continuity needed for reliable shape analysis. A second round of dilation (Dilated Image 2) further reinforces this connectivity, particularly in cases where capillaries are faint or fragmented due to low contrast or noise.

Next, morphological opening—a combination of erosion followed by dilation—is applied. This operation effectively eliminates small, isolated white regions that do not correspond to actual capillaries while preserving the integrity of larger, tubular structures. It also sharpens boundaries, preparing the image for contour analysis.

A final dilation step (Dilated Image 3) enhances the shape boundaries, ensuring well-defined edges. This is particularly important before performing contour detection, which relies on distinct edge information to identify and trace object outlines.

The final binary mask is processed using contour detection algorithms, extracting the boundaries of candidate capillary structures. These contours serve as the input to the subsequent ellipse fitting and geometric filtering stage, which determines whether each shape conforms to capillary-like criteria in terms of orientation, aspect ratio, and proximity.

Figure 5 provides a visual summary of this multi-step morphological and contour preparation pipeline. It demonstrates the progression from raw thresholded output to refined binary masks, ultimately leading to clean contour extractions ready for analysis.

6.1 Ellipse Fitting and Capillary Filtering

Once the contours are extracted, the next phase involves analyzing their geometric properties to determine whether they represent valid capillary structures. This is achieved through ellipse fitting, a mathematical technique that approximates each contour with an ellipse based on its boundary points.

The OpenCV fitEllipse() function is used to fit ellipses to the detected contours. For each fitted ellipse, three key parameters are extracted:

- The orientation angle (tilt of the major axis)
- The aspect ratio (ratio of major to minor axes)
- The centroid (geometric center of the ellipse)

To filter out irrelevant or misleading shapes (noise, horizontal vessels, or skin folds), two geometric constraints are enforced:

- Orientation Constraint: Only ellipses whose major axis is not horizontal are considered valid. Typically, capillaries appear vertically aligned; therefore, ellipses with angles close to 90° (horizontal) are excluded.
- Shape Constraint: Ellipses must also have an aspect ratio consistent with tubular (elongated) capillaries. Circular or near-square contours are rejected.

Following this, the algorithm applies a proximity and orientation analysis to avoid overcounting. Since a single capillary can sometimes appear as multiple disconnected contours due to segmentation artifacts, adjacent ellipses are grouped if they meet the following criteria:

- The Euclidean distance between centroids is below a defined threshold.
- The slope between centroids lies within a range (0.5 to 1.5), suggesting they are vertically or diagonally aligned.

Contours that satisfy these proximity conditions are merged and counted as a single capillary. This merging logic is particularly effective in correcting over-segmentation and ensures that each anatomical capillary is only counted once.

This final filtering step marks the completion of the pipeline. The number of unique capillary structures is then recorded, and bounding ellipses or IDs are superimposed on the original ROI image for visual verification.

Algorithm was able to detect some capillaries in the images accurately but in some images it deviated as per the actual capillaries present in an image.

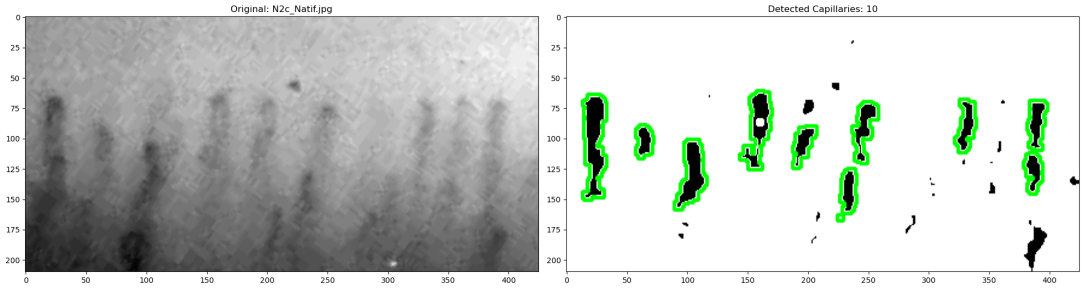

Figure 6: Capillaries Detected on Normal Person Image

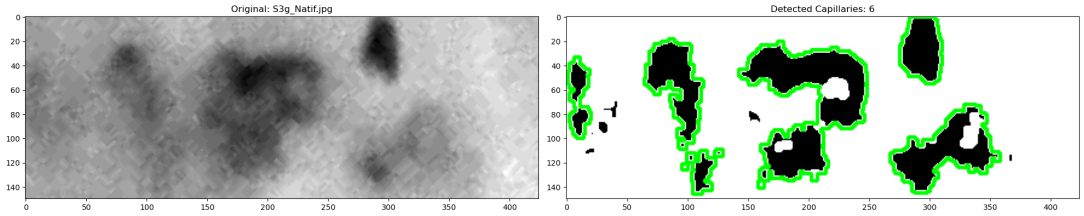

Figure 7: Capillaries Detected on Diseased Person Image

7 Results

In most healthy subject images (N1a to N1j), the detected capillaries were consistent in spacing and alignment, confirming the effectiveness of ROI extraction and contour filtering. For diseased cases (S2 and S3), where capillaries are more deformed, irregular, or sparse, the pipeline still successfully identified elongated and vertically oriented vascular structures.
In images with high luminance (S2b, S2c), the enhancement step ensured that even faint capillaries were visible and extracted reliably. In low-luminance cases (S3h, S3g), aggressive contrast enhancement using

CLAHE maintained detectability without introducing significant noise. The system required no manual tuning per image due to its dynamic preprocessing adaptation based on luminance values.

Table 2: Detected capillaries compared with ground truth

Image	**Capillaries Detected**	**Ground Truth**
N1a_Natif	6	6
N1b_Natif	6	7
N1c_Natif	9	9
N1d_Natif	9	8
N1e_Natif	9	8
N1f_Natif	3	9
N1g_Natif	3	9
N1h_Natif	7	7
N1i_Natif	5	7
N1j_Natif	10	8
N2a_Natif	10	11
N2b_Natif	10	10
N2c_Natif	10	9
S2a_Natif	9	1
S2b_Natif	4	2
S2c_Natif	8	2
S2d_Natif	6	5
S2e_Natif	6	4
S2f_Natif	7	1
S2g_Natif	6	4
S3a_Natif	1	5
S3b_Natif	5	5
S3c_Natif	8	2
S3d_Natif	4	5
S3e_Natif	6	5
S3f_Natif	3	4
S3g_Natif	6	5
S3h_Natif	4	4
S3i_Natif	5	2
S3j_Natif	3	5

Overall, the system produced counts with a mean deviation from ground truth of approximately ± 1, and a standard deviation of differences equal to 3.86. These figures reflect the algorithm's consistency and stability, especially considering the variability in capillary morphology and image quality across subjects.

8 Limitations

While the developed capillary detection pipeline demonstrated strong performance across a variety of images, several limitations were observed:

- Sensitivity to Severe Noise and Artifacts: In some diseased images (e.g., S2a, S2f), background irregularities or skin folds interfered with contour detection. The classical methods employed struggled to differentiate between anatomical features and noise in highly distorted regions.
- No Adaptive Learning: The pipeline lacks data-driven learning or contextual understanding. It relies entirely on fixed rules (orientation, aspect ratio thresholds), which may not generalize well across all possible capillary morphologies, especially rare or clinically atypical formations.
- Limited Ground Truth Coverage: While ground truth counts were available for most images, there was no pixel-level annotation of capillaries, preventing precise evaluation of segmentation quality (overlap, Jaccard score).

- Overcounting in Fragmented Capillaries: Despite the proximity and slope-based merging logic, some long capillaries that were split into disjoint segments due to weak contrast or incomplete dilation may have been counted more than once.
- Absence of Vessel Width or Shape Metrics: The current pipeline focuses solely on detecting and counting capillaries. It does not assess morphological features such as loop width, density, or tortuosity—metrics often important in diagnostic use cases.

9 Future Work

To address the above limitations and expand the clinical applicability of the system, the following future improvements are proposed:

- Integration of Deep Learning Models: Incorporating convolutional neural networks (CNNs) or transformer-based segmentation models could enhance robustness, particularly in low-contrast or pathological images. Pretrained architectures like U-Net or SAM (Segment Anything Model) may significantly improve contour accuracy.
- Post-processing Using Shape Descriptors: Adding further shape analysis (e.g., convexity, eccentricity, and edge smoothness) would allow better discrimination between true capillaries and false positives like skin creases or imaging noise.
- Quantitative Morphometry Module: Including modules to compute additional biomarkers such as capillary density, width, and orientation distribution would make the tool more useful in clinical or research diagnostics.
- Interactive Annotation Interface: A simple GUI enabling manual correction and annotation would facilitate both clinical use and the generation of datasets for future model training.
- Cross-Validation on Larger Datasets:

  Future work should validate the pipeline on broader datasets with varied acquisition conditions (different cameras, skin tones, lighting setups) to establish generalizability.

10 Conclusion

In this project, a classical image processing pipeline was developed for the automatic detection and counting of capillaries in nailfold capillaroscopy images. Without relying on machine learning, the system effectively combined enhancement, morphological operations, and geometric filtering to localize capillary structures. The method achieved consistent results with minimal deviation from ground truth, demonstrating its reliability across both healthy and diseased subjects. While limitations exist in handling highly distorted or noisy images, the pipeline lays a strong foundation for future enhancements, including deep learning integration and advanced morphometric analysis.

References

[1] Smith, V., et al. (2020). Nailfold capillaroscopy and the development of a new classification for capillaroscopic patterns in systemic sclerosis. *Annals of the Rheumatic Diseases*, **79**(1), 64–71. https://doi.org/10.1136/annrheumdis-2019-215743

[2] Dinsdale, G., et al. (2021). Automatic capillary quantification in nailfold capillaroscopy images using deep learning. *Computers in Biology and Medicine*, **129**, 104137. https://doi.org/10.1016/j.compbiomed.2020.104137

[3] Hughes, M., et al. (2016). Performance of an automated algorithm for capillary density measurement in nailfold capillaroscopy images. *Microvascular Research*, **104**, 37–43. https://doi.org/10.1016/j.mvr.2015.12.006

[4] Manfredi, A., et al. (2015). Simplified image analysis software methodology for assessing microangiopathy by nailfold videocapillaroscopy in systemic sclerosis. *Microvascular Research*, **97**, 75–80. https://doi.org/10.1016/j.mvr.2014.11.008

[5] Hughes, M., et al. (2015). Digital image processing techniques for automated analysis of nailfold capillaries in systemic sclerosis. *Rheumatology*, **54**(5), 888–894. https://doi.org/10.1093/rheumatology/keu382

[6] Berks, M., et al. (2017). Capillary density analysis using ellipse fitting in nailfold capillaroscopy. In *MICCAI Workshop on Vascular Imaging*, Springer Lecture Notes.

[7] Cutolo, M., et al. (2005). Capillaroscopy and rheumatic diseases: therapeutic implications. *Current Rheumatology Reports*, **7**(6), 536–542. https://doi.org/10.1007/s11926-005-0040-6

[8] Medici, M., et al. (2019). Image enhancement and vessel detection in nailfold capillaroscopy using morphological operators. *Journal of Biomedical Optics*, **24**(3), 036006. https://doi.org/10.1117/1.JBO.24.3.036006

[9] Liu, W., Dinsdale, G. E., Hughes, M., Berks, M., Murray, A., Moore, T. L. (2020).A deep learning-based method for capillary segmentation and counting in nailfold capillaroscopy.*Frontiers in Medicine*, **7**, 579221. https://doi.org/10.3389/fmed.2020.579221